Dynamics of Prestressed Semiflexible Polymer Chains as a Model of Cell Rheology

Noah Rosenblatt,[1] Adriano M. Alencar,[2] Arnab Majumdar,[1,3] Béla Suki,[1] and Dimitrije Stamenović[1,*]

[1]*Department of Biomedical Engineering, Boston University, 44 Cummington Street, Boston, Massachusetts 02215, USA*
[2]*Physiology Program, Department of Environmental Health, Harvard School of Public Health, Boston, Massachusetts 02115, USA*
[3]*Department of Physics, Boston University, Boston, Massachusetts 02215, USA*

(Received 10 May 2006; published 16 October 2006)

We report on a model of a prestressed nonlinear semiflexible polymer chain that links thermally driven dynamics to the creep behavior of living cells. Numerical simulations show that the chain's creep follows a power law with an exponent that decreases with increasing prestress. This is related to the propagation of free energy through the chain in response to stretching, where the propagation speed is regulated by the prestress via the chain's nonlinear elasticity. These results indicate that the main aspects of cell rheology are consistent with the dynamics of single polymer chains under tension.

DOI: 10.1103/PhysRevLett.97.168101 PACS numbers: 87.15.Rn, 87.15.−v, 83.80.Lz, 83.85.Vb

One of the outstanding problems of cellular mechanobiology is to delineate the mechanisms responsible for the rheological properties of the cytoskeleton (CSK) of adherent cells. This is important since rheological properties are fundamental for basic cellular functions (crawling, spreading, division, invasion, mechanotransduction, intracellular transport, etc.) that are essential for maintaining life. Advances in this area have been made by studying rheology of actin polymer gels [1–7], since actin is a major force-bearing component of the CSK. It was found that the rheology of actin networks is governed by the entropic dynamics of their semiflexible polymer chains [1,3,5–7]. In living cells this behavior is observed only over short time scales (<0.01 s) [8,9], whereas mechanical cellular functions operate at much longer time scales. Over longer time scales, rheological behaviors of cells scale with a weak power law [8–12]. The dynamics of glass transition has been proposed to account for these behaviors [8,10,12], but the physical basis of this theory within living cells remains unclear.

During recent years, microrheological measurements revealed that the rheology of cells is influenced by the preexisting mechanical distending stress (or prestress) borne by the CSK [8–16]. This is intriguing since it implies that dynamic processes within the cell are governed by static mechanical stress, an idea that has not been reconciled with the current approaches used to model cell rheological behaviors. In particular, it was found that the power-law exponent decreases with increasing prestress [15], regardless of cell type, rheological techniques used, and the manner by which the prestress is modulated [8,10,12–14,16].

In this study, we hypothesize that sustained mechanical tension exerted on semiflexible polymer chains by the cytoskeletal prestress alters their molecular dynamics and thereby influences cell rheology. Using a statistical mechanical model, we show that a single semiflexible polymer chain under tension exhibits properties that are similar to a variety of behaviors observed in living cells, including the power-law rheology and its dependence on the prestress.

The relaxation of linear polymer chain models follows a power law with a fixed exponent [2,5,17], unlike in living cells [8–16] and cross-linked actin gels [4]. By introducing nonlinearity in the elasticity of the polymer chain, we show that the observed dependence of the power-law exponent on the prestress can be reproduced.

We consider a chain comprised of N elastic bonds of unstretched length b_0 connected by flexible joints (''monomers'') of undeformed bond angle θ_0. Similar models have been previously used to describe elasticity of semiflexible polymers, including actin [18,19]. For simplicity, we model the chain as a two-dimensional system. Since the movement of a single chain within a polymer network is confined to a tubelike region bounded by its neighboring chains [1,17], our chain model is built and is allowed to move inside a long, straight, rigid tube of a constant diameter (d). The elastic energy (U) stored in the chain is given by

$$U = \frac{1}{2}\sum_{i=1}^{N} K_1\left(\frac{\Delta b_i}{b_0}\right)^2 + \frac{1}{4}\sum_{i=1}^{N} K_2\left(\frac{\Delta b_i}{b_0}\right)^4 + \frac{1}{2}\sum_{i=1}^{N-1} K_\theta \Delta\theta_i^2, \tag{1}$$

where K_1 and K_2 are the linear and nonlinear, ''hard'' bond stiffnesses, respectively, K_θ is the angular joint stiffness, Δb is the change in bond length relative to b_0, and $\Delta\theta$ is the change in bond angle relative to θ_0. The dynamics of the chain is driven by the motion of the joints as they thermally seek an energetically favorable position in a fixed neighborhood.

First, the chain is allowed to thermodynamically equilibrate using a Monte Carlo energy minimization procedure [20] as follows. A joint within the chain is selected and moved to a random position within a given rectangular region R. The change in energy (ΔU) of the chain with respect to the original configuration is then calculated according to Eq. (1). This procedure is then repeated M

 © 2006 The American Physical Society

times, and the configuration with the lowest ΔU is selected from these attempts. If ΔU corresponding to the selected configuration is negative, it is accepted as the new configuration. If ΔU is positive, the probability of accepting this configuration is given by $\exp(-\Delta U/kT)$, where k is the Boltzmann's constant and T is absolute temperature. This procedure is applied to each internal node of the chain in a random order which defines one Monte Carlo time step [20] that, in turn, represents a time unit in our model. In order to simulate the creep response, the chain is stretched along the tube's axis by a pair of forces (F), acting at the chain's end points. To mimic the effect of prestress, we increase F in successive steps (δF), and at each step we define the prestressing force as $F_0 = F - \delta F$. We avoid an instantaneous equilibration of the chain's end bonds in response to δF by modeling the end bonds as identical spring-dashpot-mass systems. Specifically, each end bond consists of a lumped mass (m) in series with a spring and a dashpot in parallel. The spring is a regular bond of the chain characterized by K_1 and K_2, and the damping coefficient of the dashpot is given by $2\sqrt{K_1 m}$. We perform a dynamic force balance in the direction of δF to determine the positions of the chain's ends, which is followed by a single Monte Carlo step to obtain a new chain configuration while the chain's ends are held fixed. Next, the force balance is recalculated to obtain the new end-to-end length (L) of the chain. This entire procedure is iterated in order to obtain the creep behavior by tracking the change in the component of L parallel to F (referred to as δL) as a function of time (t). Once δL reaches a steady state, the force is incremented and the creep response is recalculated.

The final calculations are carried out at a constant T, with the value of kT assumed to be unity, using the following nondimensional parameter values: $b_0 = 1$, $\theta_0 = 3\pi/4$, $d = 1.25$, $K_1 = 160$, $K_2 = 512$, $K_\theta = 1$, and nondimensional $\delta F = 20$, F_0 of 0, 20, 40, and 60, and N ranging from 16 to 2048. Additionally, we use a value of $m = 10\,000$, $M = 10$, and $R = 1.5b_0 \times 0.75b_0$. At each force step, the creep is calculated long enough ($\leq 10^6$ Monte Carlo steps) for the steady state of the chain to be reached. To test that the results are independent of M and R, we repeat the calculations by doubling or halving both parameters. We find that the rate of creep of the chain is not sensitive to the values of M and R.

The model produces creep curves that exhibit three distinct behaviors at a given F_0: an initial fast creep, a slow intermediate creep, and a steady state (Fig. 1). The intermediate creep conforms to a power law, t^α. Next, we use finite size scaling to calculate the creep response for chains of increasing N spanning 3 orders of magnitude. With increasing N, the initial creep and the power-law exponent α remain unaffected, while the duration of the power-law creep expands, delaying the onset of the steady state. To quantify the relationship between N and the duration of creep, we calculate the crossover times (t_x) between the power-law and the steady-state regimes by fitting the following ramp function to the power law and the steady-state portions of the creep curves in the log-log domain (Fig. 1):

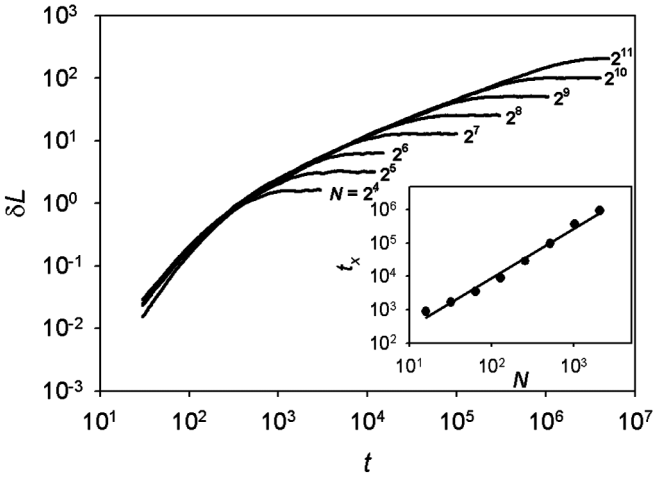

FIG. 1. Creep curves (δL vs t) of single chains of $N = 2^i$ bonds ($i = 4, 5, \ldots, 11$) and $F_0 = 20$. The creep is characterized by an initial fast response, a power-law intermediate-time response, and a steady state. The duration of the power-law regime increases with increasing N, whereas the fast response is not affected. Inset: The crossover time (t_x) between the creep regime and the steady state, calculated from Eq. (2), increases with N according to a power law $t_x \sim N^{1.49}$.

$$\log \delta L(t) = \begin{cases} A \log t + B & \forall\ 0 < t < t_x, \\ C & \forall\ t \geq t_x. \end{cases} \qquad (2)$$

The function is forced to pass through the value of δL corresponding to $t = 300$, which indicates the end of the initial creep response. We find that t_x also increases with N as a power law (Fig. 1, inset). These results indicate a consistent power-law behavior of the chain, which is ubiquitous in living cells [8–16,21].

The initial creep response of the chain is determined by the properties of its end bonds. The power-law creep, however, includes contributions from all bonds. The disturbance caused by the applied force at the end bonds is not felt instantaneously throughout the chain. To further investigate this, we calculate the creep response of internal chain segments. We find that the onsets of creep are delayed throughout the chain with segments closer to the center having longer delays and faster creep than those at the ends (Fig. 2). The cumulative effect of the delayed creep responses of the chain's internal segments leads to the observed power-law behavior. The global creep response reaches the new steady state approximately when the central segment responds to the force perturbation. In the new steady state, the chain is characterized by lower entropy, higher internal energy, and hence increased free energy, compared to the previous steady state. Thus, the creep is associated with the gradual propagation of a disturbance carrying free energy from the end bonds toward the center of the chain.

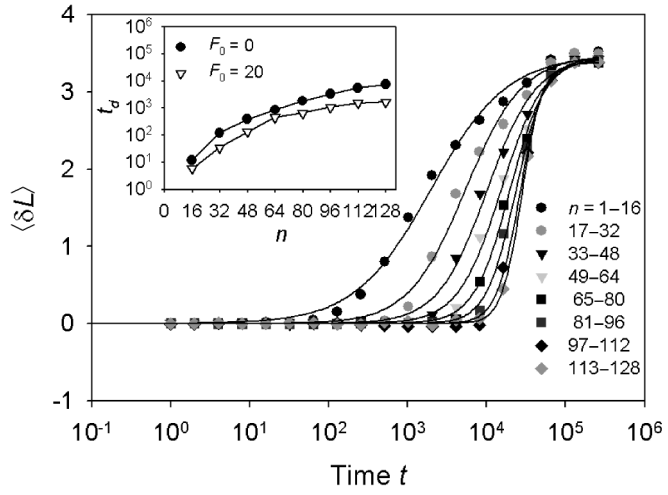

FIG. 2. Creep curves ($\langle \delta L \rangle$ vs t) of internal segments of a chain ($N = 256$), starting from the end bonds towards the center of the chain, for $F_0 = 0$; $\langle \delta L \rangle$ indicates the average end-to-end length change from over 200 simulations. Each segment contains 16 bonds; n denotes the range of bond numbers for a given segment; $n = 1$ and 256 correspond to the two end bonds, while $n = 128$ and 129 are the bonds in the center of the chain. Because of symmetry, results are shown only for half of the chain. The onset of creep is delayed in the segments closer to the center of the chain. Inset: The delay times (t_d) as a function of n for $F_0 = 0$ and $F_0 = 20$.

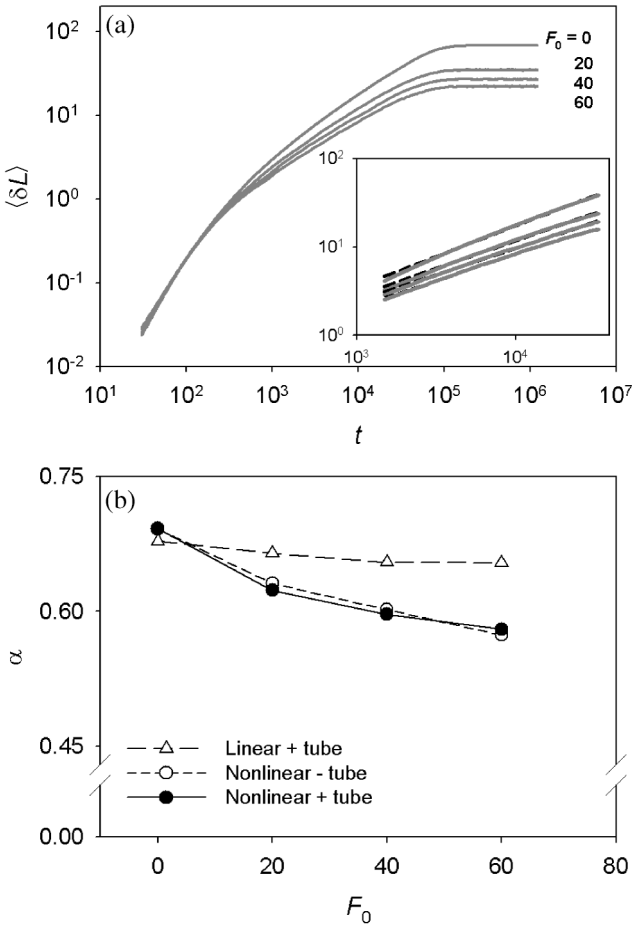

FIG. 3. (a) The rate of the creep of a chain ($N = 350$) slows down with increasing F_0 such that the power-law portions of the creep curves corresponding to different F_0's exhibit a splay with increasing time t (inset); $\langle \delta L \rangle$ indicates the mean value calculated from 5 chains. (b) For chains with nonlinearly elastic bonds, α decrease with increasing F_0, regardless of whether the chain is stretched inside (●) or outside (○) the tube. For the chain with linearly elastic bonds, α is nearly independent of F_0 (△). The values of α are obtained by fitting t^α to the power-law regime of the creep curves [black dashed lines shown in the inset of panel (a)].

Increasing F_0 causes the steady-state levels of δL to decrease, while t_x remains unchanged [Fig. 3(a)]. Consequently, both the rate of the power-law creep [Fig. 3(a), inset] and α [Fig. 3(b)] decrease with increasing F_0 similar to the behavior observed in living cells [15]. To investigate how the chain's interactions with the tube influences α, we obtain the creep of a chain outside the tube. We find that the tube has only a minor influence on the $\alpha - F_0$ relation [Fig. 3(b)]. Next, we study the effects of nonlinear bond elasticity on the creep response by comparing the $\alpha - F_0$ relation to that corresponding to a linear chain with $K_2 = 0$. We find that α is nearly independent of F_0 in the linear case [Fig. 3(b)].

To understand why nonlinear bond elasticity is critical for bringing forth the dependence of α on F_0, we analyze the internal segments' delayed creep responses (Fig. 2). Because of this nonlinearity, both the effective bond stiffness and the global chain stiffness are higher at $F_0 = 20$ than at $F_0 = 0$. Since propagation speed scales with the square root of stiffness, this should result in a faster spread of the disturbance from the end bonds toward the center of the chain. We quantify the creep of internal chain's segments, by fitting the segmental creep curves by the following function in the semilog domain:

$$\delta L(t) = \frac{h}{1 + (\tau/t)^b}. \tag{3}$$

Obtained values of the parameters h, b, and τ are then used to calculate the delayed onset of creep (t_d) defined as the time required for a segment to creep 1% of its steady-state value of δL. We find that t_d's are larger for $F_0 = 0$ than for $F_0 = 20$ (Fig. 2, inset). Thus, the leading edge of the disturbance propagates faster at higher prestresses. The increased effective chain stiffness also reduces the steady-state value of δL; at $F_0 = 0$, the steady state δL is greater than at $F_0 = 20$ (~ 3.5 vs ~ 1.6). Thus, an internal segment starts creeping earlier and attains a lower steady-state value of δL at $F_0 = 20$ than at $F_0 = 0$. Consequently, since t_x is not affected by F_0, the rate of creep of individual segments as well as of the whole chain is necessarily slower at $F_0 = 20$ than at $F_0 = 0$. Adding nonlinearity to the angular spring stiffness has the same effect on the creep behavior as the bond nonlinearity (not shown). In the chain with linearly elastic bonds, however,

the chain's effective stiffness is virtually independent of F_0, and hence F_0 has little effect on the propagation speed and thereby on α. Taken together, these findings suggest that nonlinear elasticity of single actin chains may play a key role in determining how α depends on prestress in living cells. Experiments on prestressed actin gels also indicate that material nonlinearity is necessary to link the power law to the prestress [3,4].

Our results show that the duration of the creep characterized by t_x depends on N according to a power law $t_x \sim N^z$, with $z = 1.49$ (Fig. 1, inset). Since $z < 2$, the chain dynamics is driven by faster than diffusive processes. This is also consistent with experimental data from living cells, suggesting that nanoscale dynamics of the CSK at long times is superdiffusive [11,21].

Values of α ($\sim$0.58–0.69) of the chain [Fig. 3(b)] are more than 2 times greater than the values reported for cells [8–16]. This discrepancy may reflect the arbitrary choice of model parameters. For example, reducing kT can bring α into the range of experimentally observed values.

Our results are comparable to experimental creep data for a single actin filament within actin gel [1]. The actin filament also exhibits an initial fast creep (1 s), followed by a slow creep. However, due to the short duration of the experiments ($<$3 s), a power-low regime could not be observed [1]. By comparing durations of the initial creep observed experimentally (1 s) with that of the model ($\sim$300 Monte Carlo units), we obtain a scaling factor that we use to estimate the duration of the power-law creep of the model. For a chain with $N = 32$ (Fig. 1), the power-law creep lasts $\sim$10 s, which is consistent with the power-law time scale observed in living cells [7–13]. Since the bond length of actin polymers is 5–10 nm [18,19], it follows that a chain of 35 bonds is 160–320-nm long, which is approximately the pore size of the actin cytoskeleton.

Our model links two fundamental features of cellular mechanics: prestress and power-law rheology. The results reveal that intrinsic nonlinear elasticity of the chain is essential for establishing this link. This suggests that the entropic dynamics of the chain alone cannot account for the influence of the prestress on cell rheology, and that the internal energy contributions, which result from the nonlinear elasticity, are essential. Our findings imply that the observed complexities of cell rheology already exist at the level of single prestressed polymer chains. Thus, our approach constitutes a new framework for understanding how the prestress modulates cell behavior, and represents a departure from the general thought that the cytoskeletal network properties play a primary role in determining cell rheology. Furthermore, the mechanism of the delayed propagation of a disturbance through the chain may be used to explain how mechanical signals are transmitted through the CSK. Finally, the model may also serve as a basis for describing rheology of other semiflexible biopolymers, including collagen or DNA.

We thank Mr. James Wai for his help with the numerical simulations. This study is supported by NIH Grants No. HL-33009 and No. HL-059215.

*Corresponding author.
Electronic address: dimitrij@bu.edu

[1] M. A. Dichtl and E. Sackmann, Proc. Natl. Acad. Sci. U.S.A. **99**, 6533 (2002).
[2] P. Dimitrakopoulos, J. F. Brady, and Z.-G. Wang, Phys. Rev. E **64**, 050803(R) (2001).
[3] M. L. Gardel *et al.*, Phys. Rev. Lett. **93**, 188102 (2004).
[4] M. L. Gardel *et al.*, Phys. Rev. Lett. **96**, 088102 (2006).
[5] F. Gittes and F. C. MacKintosh, Phys. Rev. E **58**, R1241 (1998).
[6] F. C. MacKintosh and P. A. Janmey, Curr. Opin. Solid State Mater. Sci. **2**, 350 (1997).
[7] F. C. MacKintosh, J. Käs, and P. A. Janmey, Phys. Rev. Lett. **75**, 4425 (1995).
[8] L. Deng *et al.*, Nat. Mater. **5**, 636 (2006).
[9] B. D. Hoffman, G. Massiera, K. M. Van Citters, and J. C. Crocker, Proc. Natl. Acad. Sci. U.S.A. **103**, 10 259 (2006).
[10] B. Fabry *et al.*, Phys. Rev. Lett. **87**, 148102 (2001).
[11] P. Bursac *et al.*, Nat. Mater. **4**, 557 (2005).
[12] G. Lenormand, E. Millet, B. Fabry, J. P. Butler, and J. J. Fredberg, J. R. Soc. Interface **1**, 91 (2004).
[13] N. Rosenblatt, S. Hu, J. Chen, N. Wang, and D. Stamenović, Biochem. Biophys. Res. Commun. **321**, 617 (2004).
[14] B. A. Smith *et al.*, Biophys. J. **88**, 2994 (2005).
[15] D. Stamenović, B. Suki, B. Fabri, N. Wang, and J. J. Fredberg, J. Appl. Physiol. **96**, 1600 (2004).
[16] X. Trepat *et al.*, Am. J. Physiol., Lung Cell Mol. Physiol. **287**, L1025 (2004).
[17] D. C. Morse, Macromolecules **31**, 7044 (1998).
[18] J. Kierfeld, O. Niamploy, V. Sa-yakanit, and R. Lipowsky, Eur. Phys. J. E **14**, 17 (2004).
[19] L. Livadaru, R. R. Netz, and H. J. Kreuzer, Macromolecules **36**, 3732 (2003).
[20] N. Metropolis and S. Ulam, J. Am. Stat. Assoc. **44**, 335 (1949).
[21] A. W. C. Lau, B. D. Hoffmann, A. Davies, J. C. Crocker, and T. C. Lubensky, Phys. Rev. Lett. **91**, 198101 (2003).